

Assessing & Mitigating Urban Heat Island in Colombo to Achieve SDG 11 and SDG 13

Bandara RMRK, De Silva MRR, Gunapraavin T and *Dissanayake DMDOK

Department of Earth Resources Engineering, University of Moratuwa, Sri Lanka

*Corresponding author – dmdok@uom.lk

Abstract

Rapid urbanization in Colombo, Sri Lanka, has intensified the Urban Heat Island (UHI) effect, raising local temperatures, increasing energy use, and stressing urban infrastructure. This study assesses spatial and temporal UHI dynamics in Colombo from 2001 to 2024 using multi-temporal satellite data, remote sensing, and GIS-based analysis. Land Surface Temperature (LST), land cover, and ecological indices (NDVI, NDBI, NBUI, UTFVI) were analyzed to identify trends and hotspots. Results show a rise in built-up areas, a decline in vegetation, and increased LST, with 39% of the city experiencing extreme heat stress, especially in dense urban cores. The study recommends increasing urban green cover, using high-albedo materials, and implementing climate-sensitive planning to align with SDGs 11 and 13. These findings provide a replicable framework for UHI mitigation and support sustainable, climate-resilient urban development in Colombo.

Keywords: Albedo, LST, NBUI, NDBI, NDVI, UTFVI

1 Introduction

In modern cities, landscapes have significantly transformed due to urbanization, altering environmental and climatic conditions. With population growth, industrial activities, and infrastructure development, Colombo has experienced rapid urbanization in recent times. This growth has increased the mean annual average temperature from around 27°C to 28.5°C over the last century [1]. As the number of man-made surfaces like buildings, roads, and pavements rises, areas of natural vegetation and open spaces decrease, resulting in the Urban Heat Island (UHI) effect [2], [3]. These surfaces absorb heat during the day and release it at night, causing urban temperatures to rise significantly compared to surrounding rural areas. This anomaly is called the UHI effect [2], [4]. The UHI effect in Colombo is worsened by its hot and humid climate, with only minimal changes aside from rainfall during the monsoon. Rising temperatures, combined with factors like high vehicle emissions and reduced vegetation,

intensify challenges in Colombo city [3]. Major challenges faced by the community include heat stress, health risks, and higher energy consumption [3]. Pollution and disrupted local climate patterns further increase UHI effects [1]. Several thermal hotspots in Colombo, such as Colombo Fort, Borella, Wellawatta, Liberty Junction, and Maradana, have significantly higher Heat Index (HI) values, ranging from 33.82°C to 40.35°C [2]. Heat stress is especially severe in April, the hottest month, exposing residents to health risks such as heat-related illness, chronic kidney disease, and cardiovascular disease [5]. As Colombo continues to grow, understanding and addressing the effects of UHI is crucial for the well-being of both residents and the environment. The growing UHI effect also impacts urban areas' durability and sustainability [6]. The Sustainable Development Goals (SDGs), introduced by the United Nations in 2015, highlight the need for

sustainable cities and climate action, with targets to ensure a brighter and more sustainable future by 2030, particularly SDG 11 (Sustainable Cities and Communities) and SDG 13 (Climate Action). It is therefore important to undertake comprehensive approaches to reduce the effects of UHI and advance urban development in recognition of the urgency of this issue. Given these challenges, this research aims to assess the spatial and temporal dynamics of the UHI effect in Colombo using advanced geospatial techniques and to propose evidence-based mitigation strategies. By exploring the interactions between urban morphology, surface temperature, and ecological health, the study seeks to inform integrated urban planning and policy interventions that support sustainable development and climate resilience in Colombo.

2 Methodology

2.1 Study Area

Colombo, the commercial capital of Sri Lanka, lies between latitudes 6°55'–6°59' N and longitudes 79°50'–79°53' E, covering approximately 37 km². The city's rapid urbanization, high population density, infrastructure development, and loss of vegetation have intensified the UHI effect, making Colombo an ideal case for UHI assessment.



Figure 1. The study area, Colombo City

2.2 Data Sources

This study utilized a multi-temporal dataset comprising five nearly cloud-free Landsat satellite images, Landsat 5 TM, Landsat 7

ETM+, and Landsat 8 OLI & TIRS captured for the years 2001, 2009, 2016, 2019, and 2024. All satellite imagery was acquired from the U.S. Geological Survey (USGS) Earth Explorer platform, preprocessed, and georeferenced to the UTM coordinate system (Zone 44N, WGS 1984 spheroid). Additional gauge temperature data for the corresponding years were sourced from the Department of Meteorology, Sri Lanka, while topographic and regional maps were obtained from the Department of Survey, Sri Lanka. Data analysis and image processing were conducted using ArcGIS Pro (version 3.4.0) and Microsoft Excel. The Landsat images provided the spectral bands necessary for land use/cover classification, land surface temperature (LST) retrieval, and the calculation of indices such as NDVI, NDBI, NBUI, albedo, and the Urban Thermal Field Variance Index (UTFVI), enabling a comprehensive assessment of the spatial and temporal dynamics of the UHI effect in Colombo.

2.3 Land Use/ Land Cover Classification

To analyze urban expansion and vegetation loss, supervised classification was performed on multi-temporal Landsat images for the years 2001, 2009, 2016, 2019, and 2024. Using the Maximum Likelihood algorithm in ArcGIS Pro, satellite bands were merged to create composite images, which were then classified into four main land use categories: built-up, vegetation, barren land, and water bodies [2].

2.4 Normalized Difference Vegetation Index

The Normalized Difference Vegetation Index (NDVI) is a widely used metric for quantifying vegetation health and density using satellite imagery. NDVI exploits the differential reflectance of healthy vegetation in the near-infrared (NIR) and red bands, and is calculated as:

$$NDVI = \frac{NIR - R}{NIR + R} \quad (1)$$

where NIR and Red represent the reflectance values in the near-infrared and red spectral bands, respectively. NDVI values range from -1 to +1, with higher values indicating dense, healthy vegetation and lower or negative values corresponding to bare soil, built-up areas, or water bodies [7].

$$UTFVI = \frac{T_S - T_{MEAN}}{T_S} \quad (4)$$

2.5 Normalized Difference Built-up Index

The Normalized Difference Built-up Index (NDBI) is designed to delineate built-up or impervious surfaces in urban environments. NDBI leverages the higher reflectance of urban materials in the short-wave infrared (SWIR) band compared to the near-infrared (NIR) band [8], and is formulated as:

$$NDBI = \frac{SWIR - NIR}{SWIR + NIR} \quad (2)$$

where SWIR and NIR represent the reflectance in the short-wave infrared and near-infrared bands, respectively. Higher NDBI values indicate built-up areas, while lower values suggest vegetation or water bodies [9].

2.6 New Built-up Index

The New Built-up Index (NBUI) is a spectral index specifically developed to enhance the extraction of built-up areas from satellite imagery, addressing the spectral confusion often encountered with traditional indices. According to Sinha (2016), NBUI demonstrates higher accuracy in delineating built-up areas compared to the Normalized Difference Built-up Index (NDBI) and Urban Index (UI). NBUI integrates information from the Short-Wave Infrared (SWIR), Thermal, Near-Infrared (NIR), Red, and Green bands, with the formula adapted for each Landsat sensor type. For Landsat 5 TM and Landsat 7 ETM+, NBUI is calculated using SWIR, Thermal band 6, NIR, Red, and Green bands, while for Landsat 8 OLI & TIRS, the formula incorporates TIRS1 (Thermal Infrared band 10). The index also includes a parameter l , which ranges from 0 to 1 depending on vegetation density, where $l=0$ for high-density vegetation and $l=1$ for low-density vegetation. The formula for NBUI, as adapted for Landsat sensors [10], [11] is:

$$NBUI = \frac{SWIR1 - NIR}{10\sqrt{SWIR1 + TIRS1}} - \frac{(NIR - Red) * (1 + l)}{(NIR + Red + l)} - \frac{(Green - NIR)}{(Green + NIR)} \quad (3)$$

2.7 Urban Thermal Field Variance Index

The Urban Thermal Field Variance Index (UTFVI) is a quantitative metric for assessing ecological vulnerability and thermal comfort in urban areas. UTFVI is derived from the ratio of the difference between local LST and the mean LST of the study area to the mean LST, as follows:

where T_S is the LST at a given point and T_{mean} is the mean LST of the entire area. UTFVI values are classified into categories ranging from optimal ecological conditions to extreme heat stress. High UTFVI values indicate areas experiencing significant thermal discomfort and ecological risk, often coinciding with dense built-up zones and minimal vegetation [2].

2.8 Land Surface Temperature Retrieval

Land Surface Temperature (LST) retrieval is a critical step in this study. Following the approach detailed by [2], the process begins by converting the Digital Number (DN) values from the thermal bands of Landsat imagery into spectral radiance using sensor-specific gain and bias values or rescaling factors. This is achieved using equations (5) or (6).

$$L_\lambda = (Grescale \times Q_{DN}) + Brescale \quad (5)$$

$$L_\lambda = \left(\frac{LMAX_\lambda - LMIN_\lambda}{QCALMAX - QCALMIN} \right) \cdot (QCAL - QCALMIN) + LMIN \quad (6)$$

where L_λ is the spectral radiance at the sensor's aperture, Q_{DN} is the quantized calibrated pixel value, and the other parameters are sensor-specific values obtained from the image metadata. The spectral radiance values are transformed into at-sensor brightness temperature (T_B) using the Planck equation and sensor calibration constants [12]:

$$T_B = \frac{K_2}{\ln\left(\frac{K_1}{L_\lambda} + 1\right)} \quad (7)$$

Here, T_B is the at-satellite brightness temperature in Kelvin, and K_1 and K_2 are pre-launch calibration constants specific to each Landsat sensor. Surface emissivity (ϵ) is estimated based on the proportion of vegetation (PV), which is calculated from NDVI values:

$$Emissivity(\epsilon) = 0.004PV + 0.986 \quad (8)$$

$$PV = \left(\frac{NDVI - NDVI_{min}}{NDVI_{max} - NDVI_{min}} \right)^2 \quad (9)$$

Where PV represents the proportion of vegetation, and NDVI is the Normalized Difference Vegetation Index. The emissivity corrected LST is retrieved by correcting the brightness temperature for surface emissivity

and the wavelength of emitted radiance using the following equation:

$$T_s = \frac{TB}{1 + \left(\lambda \times \frac{TB}{\rho}\right) \ln(\varepsilon)} \quad (10)$$

where λ is the wavelength of emitted radiance ($\lambda=11.5$), and $\rho=h \cdot c/\sigma=1.438 \times 10^{-2} \text{mK}$, with h as Planck's constant, c as the speed of light, and σ as the Boltzmann constant.

Table 1. Characteristics of Landsat TM, ETM+ & OLI/TIRS data

Acquisition Date	Satellite Type	Cloud Cover (%)	Path	Row	Sun Elevation (Degree)	Sun Azimuth (Degree)
03/14/2001	Landsat 7 ETM+	4.00	141	55	57.90309966	106.5789723
02/8/2009	Landsat 5 TM	12.00	141	55	50.49876176	124.2487089
01/27/2016	Landsat 8 OLI / TRIS	4.71	141	55	51.46836212	132.4952656
03/31/2019	Landsat 8 OLI / TRIS	1.98	142	55	62.89190086	95.28686253
01/24/2024	Landsat 8 OLI / TRIS	0.43	142	55	51.12547157	133.55251670

Table 2. Statistical data of LST Distribution in Colombo City

Satellite Sensor	Acquisition Date	Time (GMT)	Min	Max	Mean	Standard Deviation
Landsat 7 ETM+	3/14/2001	4:44:13	25.86	37.9	32.8	1.64
Landsat 5 TM	2/8/2009	4:39:37	24.6	34.67	30.85	1.34
Landsat 8 OLI/TRIS	1/27/2016	4:53:59	26.2	36.32	32.45	1.22
Landsat 8 OLI/TRIS	2019-03-31	4:59:39	28.71	40.33	35.26	1.64
Landsat 8 OLI/TRIS	2024-01-24	5:00:08	26.67	37.28	32.93	1.72

2.9 Albedo Calculation

Albedo, defined as the average proportion of solar energy reflected from the Earth's surface, is a critical parameter in assessing the thermal properties of urban environments. To accurately assess the impacts of land use changes, precise albedo measurements are crucial. Landsat 8 OLI image bands from 2019 and 2024 were used as the input for albedo calculation. The DN values of these bands were converted to Top of Atmosphere (TOA) reflectance using the reflectance rescaling coefficients available in the metadata file. This conversion was done using,

$$\rho_{\lambda} = M_{\rho} \times QCAL + A_{\rho} \quad (11)$$

where ρ_{λ} is the TOA planetary reflectance, M_{ρ} is the band-specific multiplicative rescaling factor, A_{ρ} is the additive rescaling factor, and QCAL is the quantized and calibrated pixel value. To improve the accuracy of the reflectance values, a correction for the local sun elevation angle is applied as follows:

$$\rho_{\lambda} = \frac{\rho_{\lambda}'}{\cos \theta_{SE}} = \frac{\rho_{\lambda}'}{\sin \theta_{SZ}} \quad (12)$$

where ρ_λ is the TOA reflectance corrected for the solar angle, and θ_{SE} is the local sun elevation angle (in degrees, obtained from the image metadata). This step accounts for the effect of solar geometry on reflectance measurements. Shortwave albedo (α_{short}) is then calculated using the algorithm developed by Liang and normalized by Smith, as follows [13]:

$$\alpha_{short} = \frac{0.356\rho_1 + 0.130\rho_3 + 0.373\rho_4 + 0.085\rho_5 + 0.072\rho_7 - 0.0018}{0.356 + 0.130 + 0.373 + 0.085 + 0.072} \quad (13)$$

Where ρ represents reflectance of Landsat bands 1, 3, 4, 5, and 7, except band 2 (green). The resulting albedo values are then classified into five categories based on histogram distribution.

3 Results and Discussion

3.1 Accuracy Assessment

To validate the reliability of the remote sensing-derived LST, the retrieved LST values for 2001, 2009, 2016, 2019, and 2024 were compared against daily average air temperature records from the Department of Meteorology, Sri Lanka. The error between the satellite-derived mean LST and the mean air temperature was within $\pm 2.75^\circ\text{C}$ for all years assessed, proving that the radiative transfer equation method used in this study gave sufficiently accurate LST values for UHI analysis in Colombo.

3.2 Land Use/Land Cover Distribution

LULC maps for Colombo that were produced for the years 2001, 2009, 2016, 2019, and 2024 are shown in Figure 5. Results indicate a significant reduction in barren land (from 44.13% to 6.72%) and a rapid increase in built-up area (from 44.84% to 82.81%) over the study period. Vegetation cover declined markedly, especially between 2001 and 2016. These changes are visualized in the LULC distribution maps and summarized in statistical tables for each year.

3.3 Land Surface Temperature Distribution

LST maps of Colombo city in 2001, 2009, 2016, 2019, and 2024 are shown in Figure 2. Table 2 provides a statistical description of the retrieved LST values. The highest LST values were initially concentrated around the harbor and Pettah but expanded to northern, eastern, central, and southeastern regions, including the port city project area, by 2019/2024. A

comprehensive UHI distribution map was produced by combining the areas exhibiting the highest temperature readings from each year, as shown in Figure 4.

3.4 Albedo and Urban Heat Island (UHI) Analysis

Figure 3 shows the Albedo distribution in Colombo city for 2024. The analysis between the overall UHI distribution map and the Albedo distribution map demonstrates that areas with low albedo (surfaces such as asphalt, concrete, and asbestos roofing) are major contributors to UHI formation in Colombo.

3.5 Ecological Evaluation of Colombo City

The Urban Thermal Field Variance Index (UTFVI) was calculated for 2024 to assess ecological risk and thermal stress. The UTFVI map identifies environmentally critical zones, with a substantial portion of the city experiencing "worst" thermal stress (39.21%), while 40.88% of the area maintains a healthy microclimate.

3.6 Correlation Analysis Between LST, NDVI, NBUI, and NDBI

According to the scatter plots of NDVI, NBUI, and NDBI against LST, with regression analyses and correlation coefficients summarized in Table 4. The time period taken into consideration for this study showed an inverse relation between NDVI and LST. Although the R^2 values had been not that much high, they had been statistically considerable in all five years, for the reason that p - value < 0.001 , meaning that higher NDVI values, which represent denser and healthier vegetation, correspond to lower LST values, thereby reducing surface temperatures and mitigating UHI effects. Conversely, LST and NDBI showed positive correlation coefficients each year. These correlations were statistically significant ($p < 0.001$), and the coefficients were consistently higher than those for NDVI, indicating that built-up areas have a stronger effect on increasing LST and intensifying UHI effects. Similarly, LST and NBUI demonstrated positive correlations every year, all statistically significant despite low R^2 values. This suggests that increased density of built-up areas, as captured by NBUI, also contributes to higher surface temperatures and stronger UHI impacts.

Table 3. Accuracy comparison of retrieved LST

Date	Retrieved Mean Temp (°C)	Mean Air Temp (°C)	Error
03/14/ 2001	31.91	32.00	-0.09
02/08/2009	30.38	32.10	-1.72
01/27/2016	31.95	34.70	-2.75
03/31/2019	35.21	33.20	+2.01
01/24/2024	32.93	28.60	+4.33

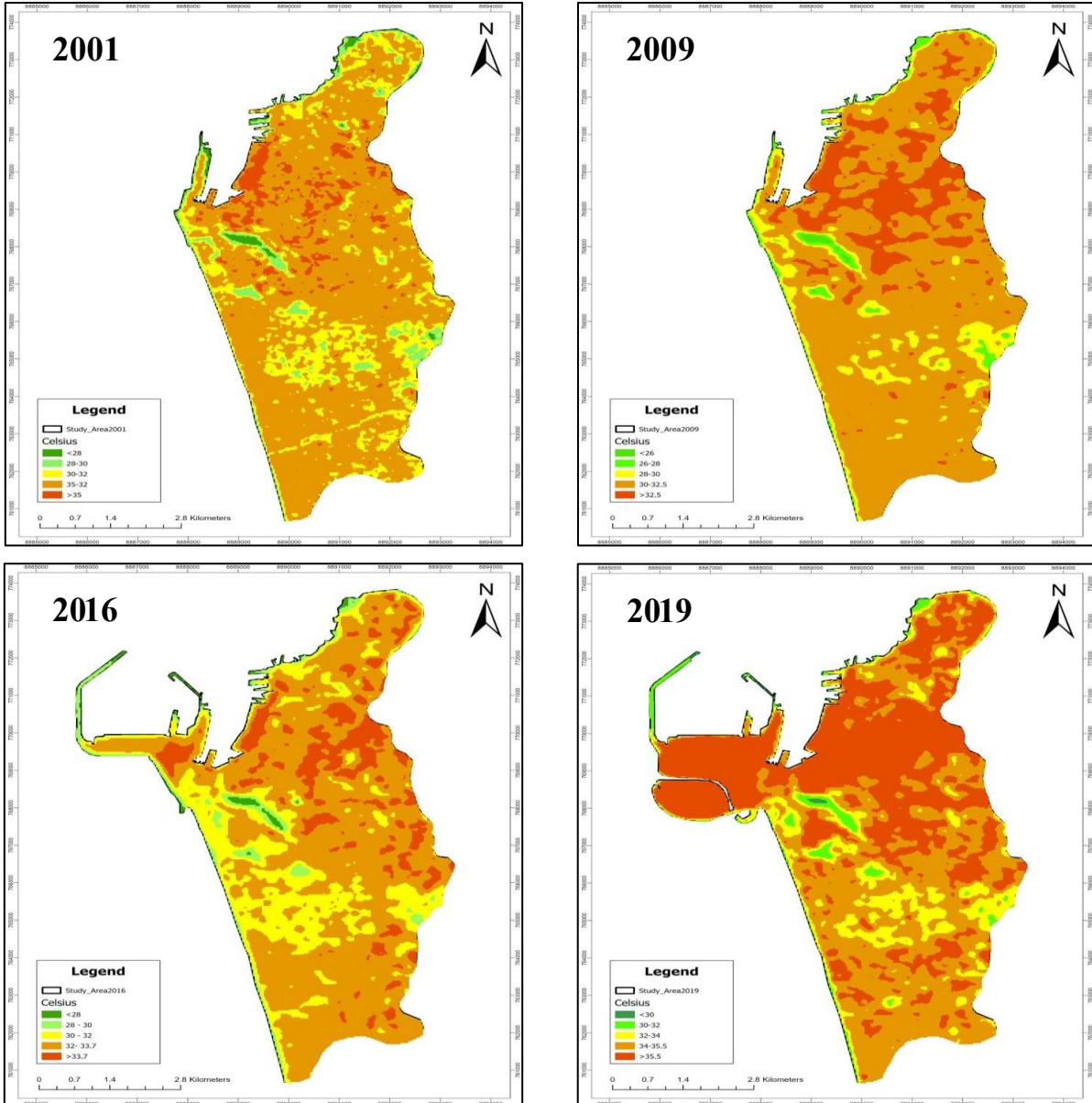


Figure 2. LST Distribution (2001-2019)

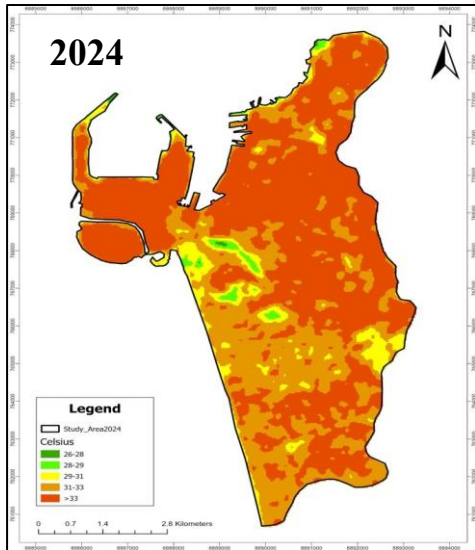


Figure 3. LST Distribution (2024)

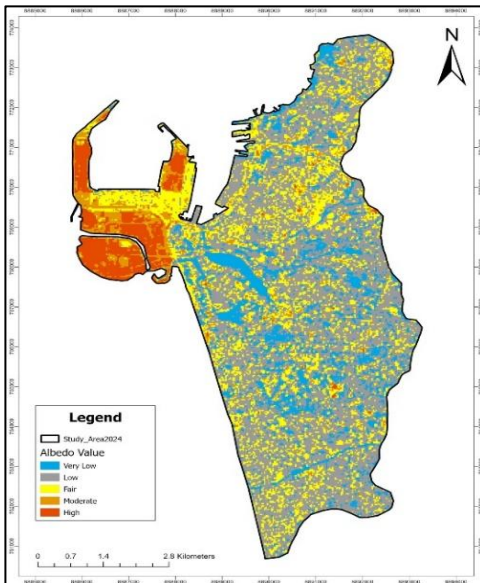


Figure 4. LST Albedo distribution in 2024

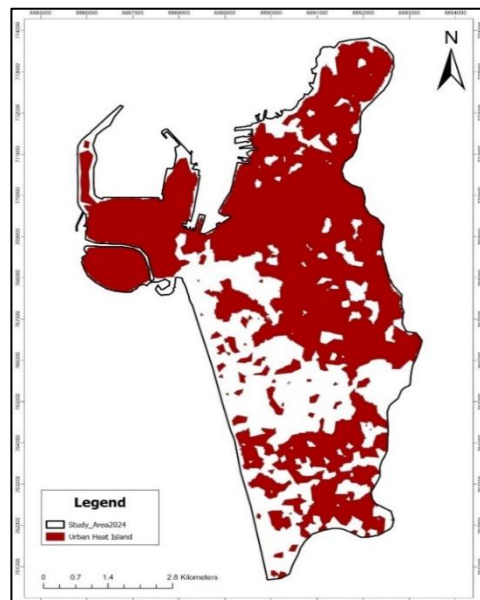


Figure 5. Overall UHI Distribution

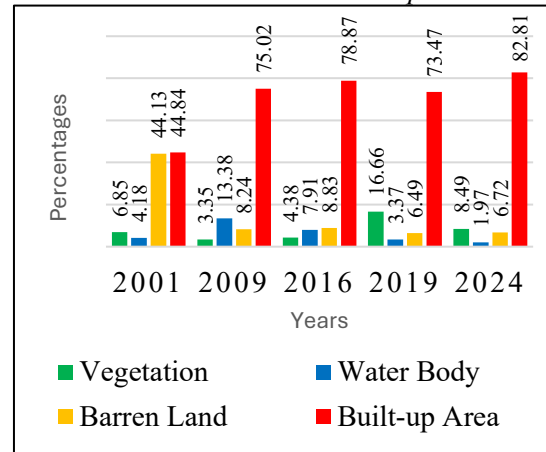


Figure 6. Land Use/Cover distribution

Table 4. Correlation Analysis results.

Correlation	LST				
	2001	2009	2016	2019	2024
NDVI	-0.542	-0.396	-0.159	-0.412	-0.294
NDBI	0.705	0.6041	0.4857	0.5757	0.593
NBUI	0.560	0.442	0.391	0.576	0.5151
Year	2001	2009	2016	2019	2024

4 Conclusion

This study discovered that the LULC pattern altered dramatically between 2001 and 2024 as a result of the town's rapid urbanization. Buildup areas are densely concentrated in the northwestern, central, and southwestern regions of the study area, with moderate distribution elsewhere. Correlation analysis confirmed that greater vegetation cover helps to mitigate UHI impacts, while denser built-up areas and low-albedo surfaces exacerbate thermal conditions. NDBI shows a stronger positive correlation with LST than NBUI, indicating that NDBI is more suitable for assessing the impact of built-up areas on land surface temperature. The UTFVI indicates that a substantial portion of the city is experiencing "worst" thermal stress (39.21%), while 40.88% of the area maintains a healthy microclimate, indicating that a substantial portion of the city is exposed to severe thermal stress and poor ecological conditions. These findings underscore the urgent need for sustainable urban planning strategies, such as increasing urban greenery, using cool roofs and pavements, enhancing ventilation, conserving water bodies, promoting environmentally friendly public transport systems, boosting building efficiency, monitoring with GIS, raising awareness, and implementing climate-resilient policies as remedial measures.

References

- [1] M. Ranagalage, R. C. Estoque, X. Zhang, and Y. Murayama, "Spatial Changes of Urban Heat Island Formation in the Colombo District, Sri Lanka: Implications for Sustainability Planning," *Sustainability*, vol. 10, no. 5, Art. no. 5, May 2018, doi: 10.3390/su10051367.
- [2] D. Dmdok and K. Kakm, "Urbanization of Colombo City and Its Impact on Land Surface Temperature from 2001-2019," *Am. J. Environ. Prot.*, vol. 10, no. 3, Art. no. 3, Jul. 2021, doi: 10.11648/j.ajep.20211003.12.
- [3] I. P. Senanayake, W. D. D. P. Welivitiya, and P. M. Nadeeka, "Remote sensing based analysis of urban heat islands with vegetation cover in Colombo city, Sri Lanka using Landsat-7 ETM+ data," *Urban Clim.*, vol. 5, pp. 19–35, Oct. 2013, doi: 10.1016/j.uclim.2013.07.004.
- [4] T. Kershaw, M. Sanderson, D. Coley, and M. Eames, "Estimation of the urban heat island for UK climate change projections," *Build. Serv. Eng. Res. Technol.*, vol. 31, no. 3, pp. 251–263, Aug. 2010, doi: 10.1177/0143624410365033.
- [5] D. Maheng, I. Ducton, D. Lauwaet, C. Zevenbergen, and A. Pathirana, "The Sensitivity of Urban Heat Island to Urban Green Space—A Model-Based Study of City of Colombo, Sri Lanka," *Atmosphere*, vol. 10, no. 3, p. 151, Mar. 2019, doi: 10.3390/atmos10030151.
- [6] M. S. P. Sumaiya, F. Ruzaik, and M. J. J. Hasmath, "Urban Heat Island phenomenon in Colombo: An analysis of its causes, impacts, and mitigation strategies," *Univ. Colombo Rev.*, vol. 6, no. 1, pp. 24–40, Jul. 2025, doi: 10.4038/ucr.v6i1.142.
- [7] K. Joon Bhang, "Anomalous Variations of NDVI for a Non-Vegetated Urban Industrial Area of Gumi, Korea," *Am. J. Remote Sens.*, vol. 2, no. 6, p. 44, 2014, doi: 10.11648/j.ajrs.20140206.11.
- [8] S. S. Bhatti and N. K. Tripathi, "Built-up area extraction using Landsat 8 OLI imagery," *GIScience Remote Sens.*, vol. 51, no. 4, pp. 445–467, Jul. 2014, doi: 10.1080/15481603.2014.939539.
- [9] X.-L. Chen, H.-M. Zhao, P.-X. Li, and Z.-Y. Yin, "Remote sensing image-based analysis of the relationship between urban heat island and land use/cover changes," *Remote Sens. Environ.*, vol. 104, pp. 133–146, Sep. 2006, doi: 10.1016/j.rse.2005.11.016.
- [10] K. Javid, M. A. Nawaz Akram, S. Pervaiz, R. Siddiqui, and N. Mazhar, "Index-based Approach in Relation to Built-up and LST Dynamics; A Study of Lahore, Pakistan," *Int. J. Econ. Environ. Geol.*, vol. 12, no. 1, pp. 32–40, Jun. 2021, doi: 10.46660/ijeeeg.Vol12.Iss1.2021.559.
- [11] School of Environmental and Rural Science, University of New England, Armidale, NSW 2351, Australia, P. Sinha, N. K. Verma, E. Ayele, School of Science and Technology, University of New England, Armidale, NSW 2351, Australia, and Department of Surveying, Dire Dawa Institute, Dire Dawa University, P.O. BOX 1362, Ethiopia, "Urban Built-up Area Extraction and Change Detection of Adama Municipal Area using Time-Series Landsat Images," *Int. J. Adv. Remote Sens. GIS*, vol. 5, no. 1, pp. 1886–1895, Aug. 2016, doi: 10.23953/cloud.ijarsg.67.
- [12] "Landsat 7 Science Data Users Handbook."
- [13] S. Zaeemdar and T. Baycan, "Analysis of the Relationship between Urban Heat Island and Land Cover in Istanbul through Landsat 8 OLI," *J. Earth Sci. Clim. Change*, vol. 8, no. 11, 2017, doi: 10.4172/2157-7617.1000423.